Doctoral Dissertation

Coulomb screening correction to the Q value of the triple-alpha process in thermal plasmas

(熱プラズマ中の３アルファ反応におけるクーロン遮蔽効果に関する研究)

Lai Hnin Phyu

Graduate School of Science, Hokkaido University

Department of Cosmosciences

2021, September

Acknowledgement

I am heartily thankful to my supervisor, Dr. W. Horiuchi, whose encouragement, guidance and support from the initial to the final level enabled me to develop an understanding of the object. I would like to thank Prof. M. Kimura for his advice and suggestions. I owe my deepest gratitude to H. Moriya for his guidance and support. I would like to show my gratitude to Prof. K. Iida, Dr. M. T. Yamashita and K. Noda. I could not have completed this work without the unwavering support of my supervisor and colleagues. It is impossible to extend enough thanks to my parents, who gave me the encouragement I needed throughout this process. Lastly, I offer my regards and blessings to all of those who supported me in any respect during the completion of this work.

Abstract

One of the most important nuclear reactions in nuclear astrophysics is the triple-alpha (^{4}He) process which leads to the formation of stable carbon, the fourth most abundant element in the universe. The first excited $J^\pi = 0^+$ state of ^{12}C, the so-called Hoyle state, plays an essential role in a triple-alpha (^{4}He) reaction. Meanwhile, this triple-alpha process may occur in weakly-coupled, thermal plasmas as encountered in normal stars. The purpose of this thesis is to investigate the changes of the Hoyle state energy due to the Coulomb screening in this weakly- coupled thermal plasma environment, which may affect the triple-alpha reaction rate. We already know that if the Coulomb potential is screened off, the repulsive force in this astrophysical environment would be less than that in a vacuum. In such a condition that a two-alpha state becomes zero energy, we expect that we would find a series of the Efimov 0^+ states might appear below the Hoyle state. First, we investigate the Coulomb screening effects on the energy shifts of the Hoyle state in a weakly-coupled thermal plasma environment by precise three-body calculations within the Debye-Hückel approximation. To reproduce the Hoyle state energy in a vacuum, we employ a three-alpha model with two kinds of three-alpha potential. To take the Debye screening in thermal plasmas into account, we use the Coulomb interaction modified in the Yukawa form. By superposing the correlated Gaussian bases, we get the precise three-body wave function of the three-alpha system. The energy shifts of the Hoyle state due to the Coulomb screening are obtained as a function of the Debye screening length. We find that our results are consistent with the conventional results based on the Coulomb correction to the chemical potentials of ions that are regarded as point charges in a weakly-coupled, thermal plasma. We have given a theoretical basis to the conventional point-charge approach to the Coulomb screening problem relevant for nuclear reactions in normal stars by providing the first evaluation of the Coulomb corrections to the Q value of the triple alpha process that produces a finite size Hoyle state. Finally, we discuss the existence of the Efimov states for the three-alpha system, which was suggested in the literature. However, we did not find these states in our calculations. The Hoyle state is still resonant state even two-alpha state becomes zero energy.

Contents

List of Figures

Chapter 1

Introduction

1.1 Properties of Nucleus

1.1.1 Discovery of Nucleus

The central core of an atom that contains all the atom's positive charges is called the atomic nucleus. Ernest Rutherford discovered the nucleus in 1911, based on the 1909 Geiger-Marsden gold foil experiment. J. J. Thomson proposed the *"plum pudding model"* of the atom before this experiment. In his model, Thomson proposed that an atom is made up of electrons that are randomly spread within a sphere of positive charge. The experiments were carried out by Hans Geiger and Ernest Marsden under the supervision of Ernest Rutherford to prove this plum pudding model. Alpha particles from a radioactive source are transmitted through a thin gold foil with a thickness of 2.1×10^{-7}m in this experiment. If Thomson's plum pudding model was true, Rutherford reasoned, the positively charged alpha particles would easily pass through the gold foil with very little deviation in their paths. However, they discovered that many alpha particles were deflected at very large angles. It was concluded that an atom has a highly dense central part where practically all of the mass and all of the atom's positive charges are concentrated in a very small region. This central part of the atom is known as the nucleus.

1.1.2 Composition of Nucleus

The nucleus is composed of protons and neutrons. Protons and neutrons have a mass of almost the same. However, a proton has one unit of positive charge ($+e$) but a neutron has no charge. These protons and neutrons are called nucleons.

The atomic number Z represents the number of protons in the nucleus while N represents the number of neutrons. The total number of nucleons, A, is represented by

$$\mathrm{A} = \mathrm{Z} + \mathrm{N}.$$

The nucleus is represented symbolically by

$$^{\mathrm{A}}_{\mathrm{Z}}\mathrm{X},$$

where, X represents the chemical element. For example, ^{12}C represents the carbon nucleus with six protons and six neutrons (12 nucleons).

1.1.3 General Properties of Nucleus

(i) Nuclear Charge

We have already known as nucleus contains protons and neutrons. So, the charge of the nucleus is equal to the number of protons in the nucleus because neutrons have no charges.

$$\text{Nuclear charge} = +Ze,$$

where, $e = 1.6 \times 10^{-19}$ C.

(ii) Binding energy

The minimum energy required to separate a nucleus into its nucleons (protons and neutrons) is known as nuclear binding energy.

$$\mathrm{BE(A,Z)} = \left[\mathrm{Zm_p + Nm_n - M(A,Z)}\right]\mathrm{c}^2,$$

where, m_p and m_n are the masses of the protons and neutrons respectively and Z and N are the numbers of protons and neutrons respectively.

(iii) Nuclear Shape and Size

A nucleus is supposed to be nearly spherical in shape. The empirical formula for the nuclear radius is $R = r_0 A^{1/3}$, where, A is the mass number and $r_0 = 1.2 \times 10^{-15}$m.

The volume of nucleus (V) is given by

$$V = \frac{4}{3}\pi R^3$$

$$\text{(or)} \quad V = \frac{4}{3}\pi r_0^3 A.$$

(iv) Average Density

Average density (ρ) can be estimated by the ratio of nuclear mass to the nuclear volume.

$$\rho = \frac{\text{nuclear mass}}{\text{nuclear volume}}$$

$$= \frac{(m \times A)}{\frac{4}{3}\pi R^3}$$

where, m is mass of one nucleon.

$$\rho = \frac{3m}{4\pi r_0^3}.$$

Putting $m = 1.66 \times 10^{-27}$ kg and $r_0 = 1.15 \times 10^{-15}$ m,

$$\rho = 2.7 \times 10^{17} \text{kg m}^{-3}.$$

This shows that the density of nucleus is very high and is almost independent with atomic number A.

(v) Nuclear Spin

In a discrete quantized orbit, the proton and neutron are in continuous motion. This orbital motion produces the nucleon with mechanical angular momentum $\vec{l}$. Nucleons have intrinsic angular momentum called spin, $\vec{s}$ in addition to orbital motion. They posses angular momentum $\vec{j}$, associated with orbital spin, $\vec{j} = \vec{l} + \vec{s}$.

1.2 Nuclear Force

1.2.1 Characteristic of Nuclear Force

We will be dealing with electromagnetic, strong, and weak interactions while dealing with the structure, reactions, and decay of nuclei. The strong or nuclear force is the primary force with which we should be concerned. In this section, we shall summarize some important features of the nuclear force.

Nuclear Force: : Inside the nucleus, the nuclear force (or nucleon-nucleon interaction) is a force that binds protons and neutrons (nucleons) together. Jame Chadwick discovered the neutron in 1932. Therefore, protons and neutrons composed the atomic nuclei. Protons, on the other hand, have a positive charge while neutrons have none. As a result, there was an attractive force inside the nucleus that could overcome the repulsive force between like-charged protons and bind protons and neutrons into a nucleus. This attractive force is called nuclear force.

The nature of nuclear force has been researched by a large number of physicists. Many experiments were carried out between 1930 and 1950 in order to better understand nuclear force. Hideki Yukawa [1] was the first to attempt to describe the nature of nuclear force in 1934. The nuclear force was conceived to be transmitted via particles known as massive bosons (mesons), according to his hypothesis. The Yukawa potential is a potential of the form

$$V_{\text{Yukawa}}(r) = -g^2 \frac{e^{-\mu r}}{r},$$

where, g is a magnitude scaling constant, ie., the amplitude of potential, μ is the Yukawa particle mass and r is the radial distances to the particles. The constants are determined empirically.

After Yukawa potential, the first semi-empirical quantitative models, such as the Wood-Saxon potential [2], were suggested in the mid-1950s (1954). Following that, there was significant progress in both experiment and theory.

1.2.2 Features of Nuclear Forces

Some key observations and/or features of nuclear force are written below.

The nuclear force is known to be very attractive, binding nucleons together to create a densely packed nucleus. When the distance between nucleons is around 1 fm (Femtometer), the nuclear force is very attractive. The attractive nuclear force is stronger than the repulsive Coulomb force between protons at this distance. It is able to overcome the repulsion of the protons in the nucleus. When protons are separated by more than 2 to 2.5 fm, Coulomb repulsion becomes the only relevant force between them. As the distance between the protons exceeded 2.5 fm, the attractive force began to rapidly decrease.

Experiments with the scattering of high-energy particles from nuclei have revealed that the nuclear force contains a repulsive core. The nuclear force becomes repulsive at small nucleon separations (less than 0.7 fm). The total binding energy of the nucleus is just proportional to the number of nucleons. This fact indicates the short range nature of the nuclear force. Each nucleon only interacts with its nearest neighbours, therefore it sees the same environment regardless of the number of nucleons at a larger distance. As a result, the nuclear force is saturated. Another property of the nuclear force between two nucleons is charge-independent. So, the strong interaction between two protons, two neutrons, or between a proton and a neutron is almost the same. Nucleon-nucleon scattering and the binding energies of light nuclei provide evidence for the charge independence of nuclear forces.

The deuteron is the simplest bound nuclear system, consisting of a neutron and a proton. The deuteron has a quadrupole moment of 0.00286 barns (0.286 fm^2), indicating that it is not exactly spherical and that the force between two nucleons is not spherically symmetric. Formally, the force between two nucleons is divided into two parts: a spherically symmetric central force and an asymmetric tensor force that depends on the angles between each nucleon's spin axis and the line connecting them.

It is reasonable to assume that the ground state of the deuteron, like the ground state of the hydrogen atom, has zero orbital angular momentum. Because the total angular momentum is one unit of $\hbar$, it follows that the spin angular momentum is one unit of $\hbar$, implying that the proton and neutron spins are parallel. The conclusion is that if two nucleons' spins are antiparallel, they are not bound together, which is compatible with the fact that there are no proton-proton or neutron-neutron bound states. The Pauli exclusion principle forbids the bound parallel spin state in the case of identical particles. So the nuclear force is spin-dependent. These are some important features of nuclear force.

1.3 History of α-cluster

Nuclear clustering is one of the most interesting and important aspects of many-body dynamics, and it may be seen in a wide range of physics systems. Clustering has long been thought to play an important role in the structure of the ground and excited states of $N{=}Z$ nuclei. The saturating two-nucleon force and the Pauli exclusion principle enhance the cluster formation in nuclear systems, particularly in light nuclei. The cluster models predict that some of the observed energy levels can not be explained by free nucleons interacting with each other, but rather by the nucleons clumping together into clusters, and it is mainly the clusters that interact with each other.

Because of the unique characteristics of α-clusters, or ^{4}He nucleus, which are made up of two protons and two neutrons, α-clusters are the most important and fundamental of the clusters. It is exceptionally stable with a binding energy of 7.07 MeV/nucleon. Cluster structures in nuclei have been researched for a long time, dating back to the discovery of the neutron. Following Gamow's α-decay hypothesis [3], it was only reasonable to look into a model in which nuclei are made up of α-particles. Gamow explained a very detailed theory of the properties in his book *"Constitution of Nuclei"* [4], which was published in 1931. He hypothesized that $4n$-nuclei like ^{8}Be, ^{12}C, ^{16}O, and so on, were composed of α-particles while protons and electrons as well as α-particles made up the other nuclei. He also recognized that the nuclear 'electrons' had peculiar properties and wrote: *"For some unknown reason, although the electrons in the nucleus behave in a peculiar and obscure way, this does not affect very much the laws governing the motion of the nuclear α-particles and protons; we can treat nuclear processes involving only α-particles and protons independently of the nuclear electrons"*.

Hafstad and Teller [5] published *"The alpha-particle Model of the Nucleus"* in 1938, establishing a simplified theory based on the special properties of the so-called alpha-conjugate nuclei, of which the stable ones are ^{12}C, ^{16}O, ^{20}Ne, ^{24}Mg, ^{28}Si, ^{36}Ar and ^{40}Ca. Ikeda and colleagues proposed a threshold picture, which is shown in Fig. 1.1, for the appearance of cluster states thirty years later [6]. Ikeda has proved to be very powerful in identifying situations in which cluster structure can be observed. This diagram illustrates possible cluster structures that could exist in excited states of light nuclei, and it proposes that particular clusters will emerge at excitation energies near the corresponding decay threshold. Indeed, some rotational bands or states for the low-excitation-energy region in light α-conjugate nuclei can be easily understood from the view of cluster structures, whereas they are difficult to explain from the shell-model picture.

Resonating group method (RGM) [7, 8], generator coordinate method (GCM) [9], orthogonality condition model (OCM) (semi-microscopic cluster model) [10] and macroscopic cluster model, which takes into account the effect of the antisymmetrization and Pauli principle, are four important and representative cluster models. These models have successfully reproduced several experimental data related to clustering in $4n$ light nuclei.

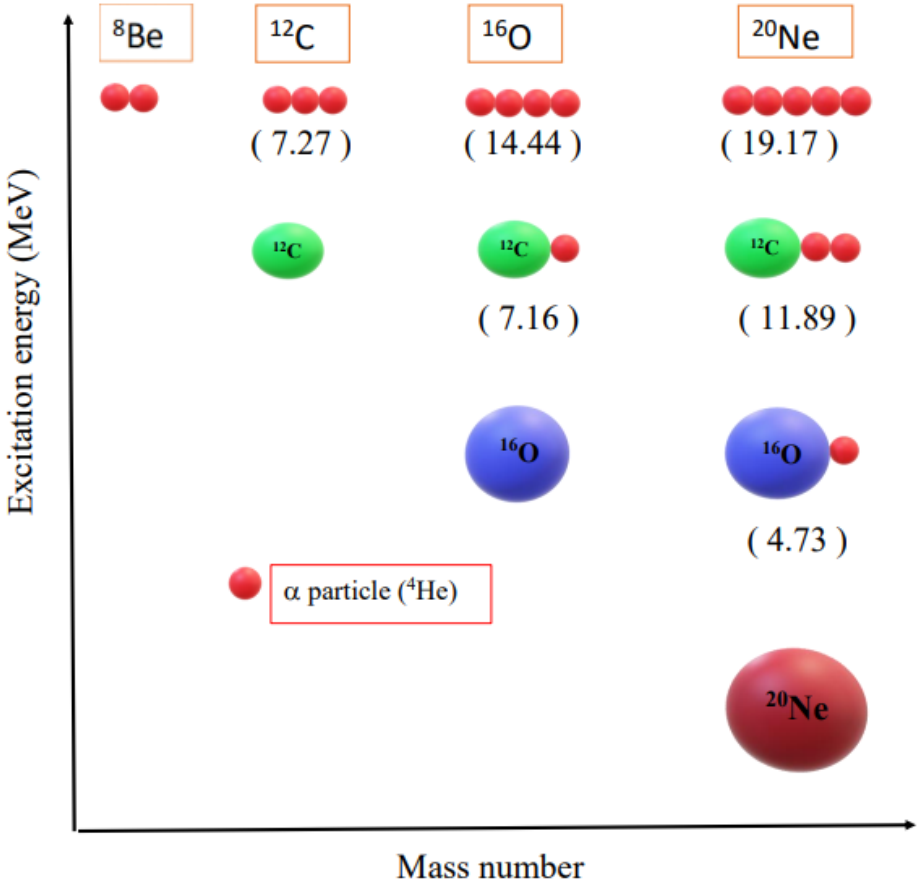

Figure 1.1: Ikeda diagram

1.3.1 three-alpha system (^{12}C)

The structure of the ^{12}C spectrum has been one of the most interesting phenomena in nuclear physics in recent decades (see Refs. [11, 12, 13]). Understanding nucleosynthesis in normal stars [14, 15, 16, 17], where ^{12}C is formed in the fusing of three ^{4}He nuclei (α particles) through the formation of the ^{8}Be resonant state as an intermediate state [18], requires an accurate description of the production process of the ^{12}C element, which is one of the most abundant elements.

In 1939, Bethe had concluded that the formation of ^{12}C from the collision of three α-particles within stars was highly improbable, concluding that a temperature some 50 times higher than that known within stars such as the Sun was required [19]. Öpik took the first significant step forward in 1951 who recognized that elevated temperatures were possible in stars in the red giant phase [20]. In 1952, Salpeter [18] suggested that rather than the direct simultaneous capture of 3-α particles, a sequential process is preferred

$$^{4}\mathrm{He} + {}^{4}\mathrm{He} \rightarrow {}^{8}\mathrm{Be}$$
$$^{8}\mathrm{Be} + {}^{4}\mathrm{He} \rightarrow {}^{12}\mathrm{C} + \gamma.$$

Figure 1.2 shows the schematic of the decay process by which ^{12}C is formed from the radiative ^{8}Be + ^{4}He capture. However, because of the low density of ^{8}Be, triple-α reaction has a very low rate. Then Hoyle claimed that, in order to explain the measured abundance of carbon in the universe, this reaction must take place through a hypothetical ^{12}C resonance, strongly enhancing the cross section. Hoyle suggested that this resonance is a $J^{\pi} = 0^{+}$ state at $E_{\gamma} = 0.4$ MeV. Subsequent experiments indeed found a 0^{+} resonance in ^{12}C in the predicted energy region. It is the second 0^{+} state (0_{2}^{+}) and the second excited state of ^{12}C. This state, which is called the Hoyle state [21], was experimentally confirmed soon afterwards [22] and has been believed to play an essential role in increasing the production rate of ^{12}C.

The ground state of ^{8}Be being unbound to decay to two α-particles by 92 keV, as indicated in the Ikeda diagram shown in Fig. 1.1 [6], may have a well-developed α-cluster structure. As shown in the Ikeda diagram, the ^{8}Be + α decay threshold, or equivalently 3α decay threshold (7.274 MeV), would allow the internal excitation energy to be transformed into the binding energy of the clusters. This raises the idea that the optimal conditions for the transformation of the ^{12}C nucleus into a sub-structure of three-α particles exist close to the region occupied by the Hoyle-state. In other words, the fact that the Hoyle-state has a three α-cluster structure could explain why it exists at an energy just above the α-decay threshold. In turn, it is the link between the clustering and threshold which is the remarkable coincidence that lies behind the origin of the abundance of ^{12}C.

The structure of the ground and excited states of ^{12}C nucleus has been studied using microscopic, macroscopic, and semi-microscopic cluster models. In particular, the microscopic 3-α calculation was performed within the resonating group method (RGM) by Kamimura [7, 8] and within the generator coordinate method (GCM) by Uegaki [9]. For

the ground state of the ^{12}C and some excited states, both calculations yield reasonable results. These models' wave functions, on the other hand, are complicated to handle.

The ^{12}C nucleus was also studied using macroscopic models. Clusters are treated as structureless particles in these models, interacting through local potentials to reproduce the experimental α-α phase shift. However, α-α potential is not local due to the antisymmetrization. Furthermore, any reliable results on the structure of low-lying states of the ^{12}C nucleus required a precise elimination of the Pauli-forbidden states. Ref. [10] introduced the Orthogonality Condition Model (OCM) as an approximation of the resonating group method and used it to investigate the 3-α structure in ^{12}C. In OCM, the inter-cluster wave function is required to be orthogonal to the forbidden states and, thus, the later states are completely removed from the wave function. In 2-cluster systems, OCM permits only eigenfunctions of the antisymmetrization operator to be obtained, rather than eigenvalues, which enter the Schrodinger equation and so affect the dynamics of the cluster system. As a result, a part of exchange effects is absent in OCM, even though it may be essential, particularly in 3-cluster systems. This is supported by the fact that the lack of binding energy of ^{12}C is observed in OCM compared to RGM calculations.

Our present work aims to explore the Coulomb screening effect of the 0_2^+ state in ^{12}C. So in the next section, we will introduce the Hoyle state of ^{12}C.

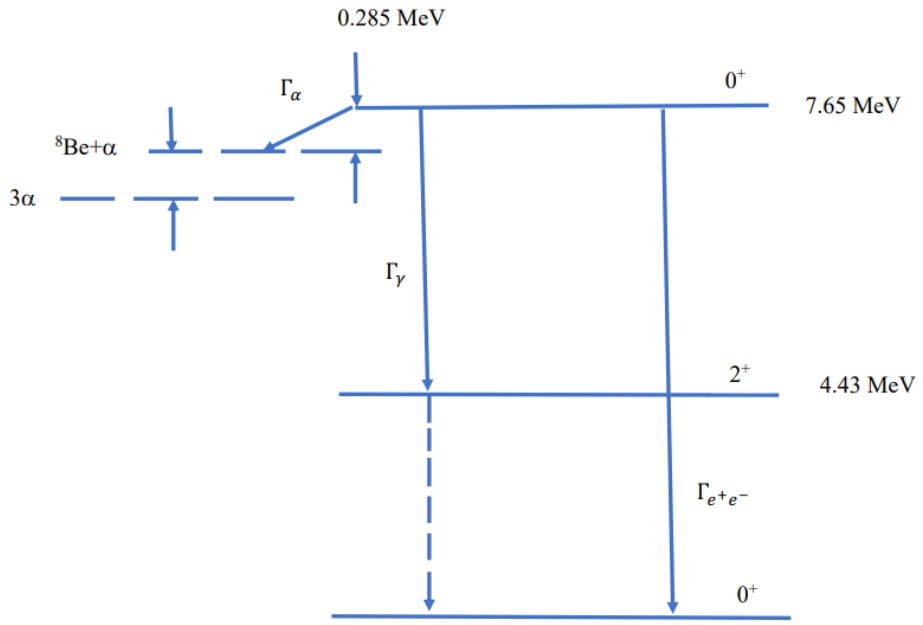

Figure 1.2: Schematic of the decay process by which ^{12}C is formed from the radiative ^{8}Be + ^{4}He capture.

1.3.2 Hoyle state of ^{12}C

The so-called "Hoyle state", which is a prototype of α cluster states in light nuclei, plays a prominent role in a nuclear structure. The fact that this state is extremely near the three-α threshold, and that the α particle is strongly bound to make it probable. As a result, the wave function of 0_2^+ contains a dominant three-α clustering nature. In several macroscopic and microscopic three-α models, the low-lying states of ^{12}C, including 0_2^+, are investigated. In fact that the Hoyle state plays a crucial role in nucleosynthesis and may have a cluster-type structure that is linked to the nature of strong interaction, implying that there is a connection between the observed abundance of ^{12}C at every level. Therefore, the Hoyle state has become a benchmark for nuclear astrophysics, nuclear structure, and nuclear forces. It is undeniable that understanding the nature of this state may, in principle, solve many problems simultaneously. The Hoyle state has even been used to constrain the running light quark masses [23]. It is also possible that the bosonic nature of the α-particle indicates that the Hoyle state is associated with nuclear matter, where the important degree of freedom is bosonic rather than fermionic–similar to an atomic Bose-Einstein Condensation (BEC) [24]. So the studying of the Hoyle state of ^{12}C is very important for nuclear structrue. In our thesis, we will also study the changes of Hoyle state energies due to the Coulomb screening in thermal plasma environment.

1.3.3 Coulomb Screening in thermal plasma environment

According to Ref. [25], X-ray bursting occurs as a result of a thermonuclear explosion in a neutron star's accreted shell. A cold and dense plasma environment can be formed in the outer layer of this X-ray burst. A plasma composed of helium ions and electrons appears in this environment, which is shown in Fig. 1.3. In our thesis, we will use this plasma environment to investigate the Coulomb screening effect on the Hoyle state. Now we will explain what Coulomb screening is and how it impacts the triple-alpha reaction rate in this plasma environment. The fully ionized plasma is obtained when the environment reaches the temperature $T \sim 10^8$ K and $\rho \sim 10^6$ gcm^{-3}. In this plasma, the free electrons and helium ions interact via the Coulomb potential. When the two helium ions approach each other with the possibility of engaging in a nuclear reaction, a screening cloud (consisting of protons and electrons) surrounds each ion. Each helium ion could be attracted by the electrons in this screening cloud. The helium ion would be repelled by the protons. So Coulomb screening is caused by these two effects of the particles in the screening clouds on the potential energy of the helium ion pair. The surrounding degenerate electrons reduce the standard Coulomb potential between approaching ions in the plasma to a screened potential. This Coulomb screening phenomenon can impact the triple-alpha reaction rate.

Now we will go through the concept of screening energy in more detail. In 1954, Salpeter [26] derived an expression for the enhancement of nuclear reaction rates due

to electron screening. In his paper, he explained the main points of the weak screening and strong screening in plasma. However, we are only interested in the weak screening. As a result, we will go over the conditions for weakly screening. Salpeter solved the Poisson-Boltzmann equation for electrons and ions in plasma under the condition of weak screening to get an expression for the screening energy. This expression is similar to screening energy of the Debye-Hückel theory of dilute solutions of electrolytes [27],

$$E_{\text{screen}} = \frac{4e^2}{\lambda_D}$$

where, the Debye length, λ_D, is the screening length of a plasma at temperature T and n is the number density. The Debye screening length is

$$\lambda_D = \left(\frac{k_B T}{4\pi e^2 (n_e + 4n_\alpha)} \right)^{1/2}.$$

So, this screening length (λ_D) will be used in our thesis to investigate the Coulomb screening effect. In the next chapter, we will explain the details of Debye screening length.

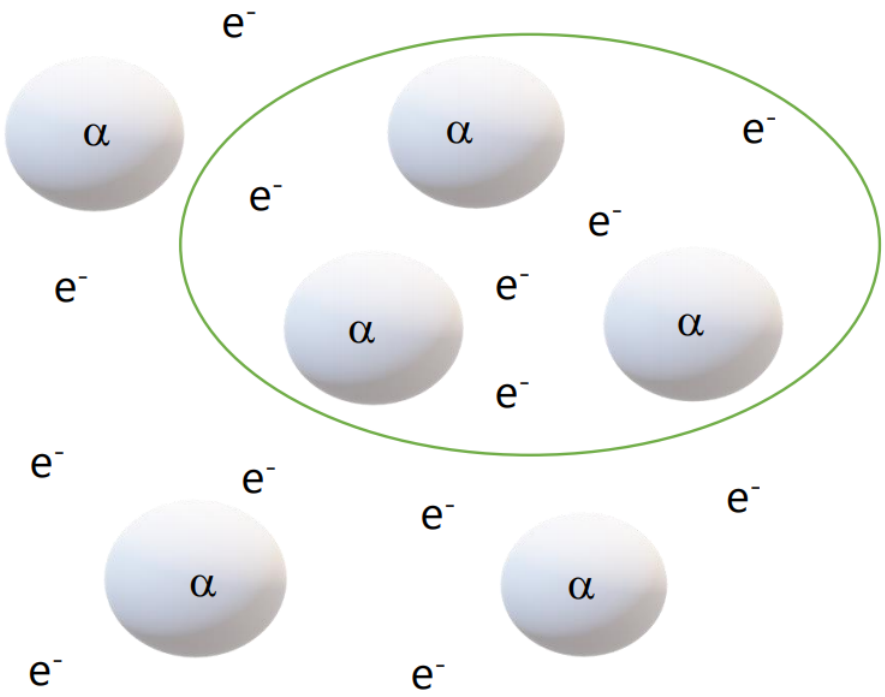

Figure 1.3: Three-alpha particles in plasma environment

1.3.4 Efimov effect in three-alpha system

The Efimov effect is a universal quantum phenomenon that can be found in many fields of physics. Vitaly Efimov discovered an interesting effect in the quantum spectrum of the three particles in 1970 [28, 29]. In his calculations, the particles interact through short-range attractive interactions, implying that the interaction potential is dependent on the separation between the two particles, r. This short-range attractive interaction is nearly resonant, which means the attractive interactions can just barely support a weakly two-body bound state. In this situation, Efimov pointed out that the two-body interaction is said to be resonant when the scattering length of S-wave, $|a|$, is sufficiently larger than the interaction range, l. This is because the two particles are scattered at low energy during their collision, which is very close to binding. According to Efimov's paper [28, 29], when another particle is added to this two-particle system, the long-range three-body force emerges. And beyond the range of interactions, this attraction may support an infinite series of three-body bound states. These states are known as Efimov states or Efimov trimers, wherein the three particles are bound at larger distances. The particles going back and forth from one another explain the Efimov attraction. Efimov attraction holds these particles together. A detailed explanation of the Efimov effect can be found in Ref. [34].

Efimov proposed that the Hoyle state may be explained as a universal trimer of alpha particles (i.e. helium nuclei, which are bosons) bound by the Efimov attraction in his original papers [28, 29]. When electromagnetic interactions are turned off, it can be thought of as an expansion around the limit; the ^{8}Be ground state is exactly at the threshold and displays conformal invariance. The Hoyle state in ^{12}C would appear as a remnant of an excited Efimov state in this situation. So in our calculations, we will investigate this Efimov effect in Hoyle state by using the screened Coulomb potential. The detailed calculations are explained in the next chapter.

1.4 Motivation

In our thesis, we have done three main parts. Firstly, we calculate the energies of the ground state and Hoyle state of ^{12}C. We perform the precise three-body calculations with the correlated Gaussian expansion to get the energies of ^{12}C. In our calculations, we use the macroscopic cluster model. The three α particles are considered as the structureless point particles in this model. We use the two-body modified Ali-Bodmer (AB) potential and three-α potentials to reproduce the empirical ^{8}Be, ground state, and Hoyle state energies [15]. After obtaining the energies of the ^{12}C, we consider that if the Coulomb potential is screened off, what will happen? To know this effect, firstly, we will consider the plasma environment as encountered in a normal star that undergoes a stable burning of helium. In this environment, we study the Coulomb screening effect on the Hoyle state. We employ the same two- and three-α potentials to get the screened Hoyle state energies of ^{12}C. To understand the Coulomb screening effect on Hoyle state in a weakly-coupled thermal plasma, we use the Coulomb interaction in the Yukawa form instead of the standard Coulomb potential. This form is relevant as long as the Debye-Hückel approximation is valid. This approximation well explains the long-range Coulomb screening in a weakly-coupled thermal plasma.

This screening reduces the Coulomb interaction between α particles and this astrophysical environment would make it less repulsive than that in free space. We also search the possible Efimov states [32, 33] for the three-alpha system due to the Coulomb screening effect. The works of Higa and Hammer based on the effective-field theory look into the effect of the Coulomb interacts with alpha systems close to unitarity. It was concluded that due to the nature of the Hoyle state, which appears as the three-α first excited state, a series of the Efimov 0^+ states might appear above the Hoyle state in possible astrophysical environments where the two-α ground state energy would become almost zero. In Ref. [34], the authors explain the above situation that excluding the Coulomb repulsion, the nuclear force between the two alpha particles does not seem to be resonant. So, the resonance condition may not be satisfactory. This would suggest that the attraction between the alpha particles is directly due to the nuclear force rather than the Efimov attraction. Another point is that even if the α-α interaction is resonant, the Efimov attraction seems too weak to overcome the Coulomb repulsion and support a resonant state at distances larger than the interaction range l. Therefore, only full treatment of the three-body problem with short-range and Coulomb interactions could shed some light on the hypothesis that the Hoyle state could become an Efimov state. To explain this effect, we investigate the Efimov state in ^{12}C by using the screened Coulomb potential.

This thesis is organized as follows. The theoretical calculations of the three-alpha system are explained in Chapter. 2. First, we explain how to construct the wave function and the Hamiltonian of the three-alpha system. Then we describe the Coulomb screening

correction to the Hoyle state energy in a weakly-coupled thermal plasma. This section also discusses the validity of the screened Coulomb potential. In Chapter. 3, we show the calculated results for the energy shifts of the Hoyle state due to the screening and compare them with those based on the Coulomb correction to the chemical potential of the point ions in the weakly-coupled thermal plasma. Conclusions are drawn in Chapter. 4.

Chapter 2

Theoretical Framework

2.1 Screening correction to triple-alpha reactions in the point-charge approximation

In this section, we will explain how to derive the Debye screening length and screening correction to triple-alpha reactions in the point-charge approximation.

2.1.1 Debye screening length

We will explain what the Debye screening length is and how to calculate it using the Gauss' law [27]. The most important physics parameter for describing a plasma is the Debye screening length. The Debye screening length is the distance over which charged particles are able to screened out the electrostatic potentials. A charge in plasma attracts the opposite charge and repels like charges. As a result, the charges it has attracted screen its electric field. The particles outside the screening charges are unaware of the inside charge's presence.

Now, we will use the Gauss' law to get the Debye screening length. In a system of N different species of charges, the i-th species carries the charges q_i and has the number density n_i. These charges are distributed in a continuous medium that is characterized only by its relative static permittivity, ε_r. The Gauss' law is satisfied by the electric potential $\Phi(\boldsymbol{r})$ caused by the distribution of charges within this medium:

$$\varepsilon \nabla \cdot \mathbf{E} = \sum_{i=1}^{N} q_i n_i, \tag{2.1}$$

where $\varepsilon \equiv \varepsilon_r \varepsilon_0$, ε_0 is the electric constant. And we have $\mathbf{E} = -\nabla\Phi(\boldsymbol{r})$, so the Gauss' law becomes

$$\varepsilon \nabla^2 \Phi(\boldsymbol{r}) = -\sum_{i=1}^{N} q_i n_i. \tag{2.2}$$

This is Poisson's equation.

The mobile charges not only help to establish $\Phi(\boldsymbol{r})$ but they also move in response to the Coulomb force, $q_i \nabla\Phi(\boldsymbol{r})$, that is present. We will assume that the ions and electrons have the same temperature T and number density n for this calculation. So the number density of the i-th charge species is described by the Boltzmann distribution,

$$n_i = n_i^0 \exp\left(-\frac{q_i\Phi(\boldsymbol{r})}{k_B T}\right), \tag{2.3}$$

where, k_B is the Boltzmann's constant and n_i^0 is the mean number density of charge of species i. The Poisson-Boltzmann equation is obtained by identifying the instantaneous concentrations and potential in the Poisson equation with their mean-field counterparts in Boltzmann's distribution.

$$\varepsilon\nabla^2\Phi(\boldsymbol{r}) = -\sum_{i=1}^{N} q_i n_i^0 \exp\left(-\frac{q_i\Phi(\boldsymbol{r})}{k_B T}\right). \tag{2.4}$$

By assuming that the potential energy of the particles in the applied field is significantly smaller than their thermal energy, we may reduce this second-order nonlinear differential equation: $q_i\Phi(\boldsymbol{r}) \ll k_B T$. So we can solve the right hand side of Eq.2.4 by a Taylor expanding the potential:

$$\exp\left(-\frac{q_i\Phi(\boldsymbol{r})}{k_B T}\right) \approx 1 - \frac{q_i\Phi(\boldsymbol{r})}{k_B T} \tag{2.5}$$

This approximation yields the linearized Poisson-Boltzmann equation

$$\varepsilon\nabla^2\Phi(\boldsymbol{r}) = \left(\frac{\sum_{i=1}^{N} n_i^0 q_i^2}{k_B T}\right)\Phi(\boldsymbol{r}) - \sum_{i=1}^{N} n_i^0 q_i \tag{2.6}$$

which is also known as the Debye-Hückel equation. For electrically neutral systems, the second term on the right-hand side vanishes. So the Eq.2.6 becomes

$$\nabla^2\Phi(\boldsymbol{r}) = \left(\frac{\sum_{i=1}^{N} n_i^0 q_i^2}{\varepsilon k_B T}\right)\Phi(\boldsymbol{r}). \tag{2.7}$$

To solve the above second-order differential equation, we define $K^2 = \frac{\sum_{i=1}^{N} n_i^0 q_i^2}{\varepsilon k_B T}$.

$$\nabla^2\Phi(\boldsymbol{r}) = K^2\Phi(\boldsymbol{r}). \tag{2.8}$$

But $\nabla^2\Phi(\boldsymbol{r}) = \frac{1}{r^2}\frac{d}{dr}\left(r^2\frac{d\Phi(\boldsymbol{r})}{dr}\right)$. So we obtain

$$\frac{1}{r^2}\frac{d}{dr}\left(r^2\frac{d\Phi(\boldsymbol{r})}{dr}\right) = K^2\Phi(\boldsymbol{r}) \tag{2.9}$$

and this differential equation has the general solution

$$\Phi(\boldsymbol{r}) = A\frac{e^{-Kr}}{r} \tag{2.10}$$

where, $K = \left(\frac{\sum_{i=1}^{N} n_i^0 q_i^2}{\varepsilon k_B T}\right)^{1/2}$. The Debye screening length is defined as

$$\lambda_D = \left(\frac{\varepsilon k_B T}{\sum_{i=1}^{N} n_i^0 q_i^2}\right)^{1/2}. \tag{2.11}$$

For vacuum, we assumed that $\varepsilon_r = 1$. So the Debye screening length becomes

$$\lambda_D = \left(\frac{k_B\, T}{4\pi e^2 (n_e + \sum_i\ n_i Z_i^2)}\right)^{1/2}, \tag{2.12}$$

where $Z_i = \frac{q_i}{e}$ is the charge number of ions of species i.

We will study how the Coulomb screening impacts the energy shifts of the Hoyle state in a weakly-coupled thermal plasma using this Deby screening length.

2.1.2 Screening correction to triple-alpha reactions in the point-charge approximation

In this chapter, we will explain the Coulomb screening by following the conventional approaches. In this calculation, we assume that all the ions involved, including a ^{12}C nucleus in the Hoyle state, are point charges. Then we estimate how much carbon is produced via triple-alpha reactions as encountered in normal stars that undergo stable burning of helium. In helium burning, the temperature T is of the order of or even higher than 10^8 K and the mass density ρ is typically 10^3–10^6 g cm^{-3}. So, in this environment, the Hoyle state (C*) occurs via two successive steps: Firstly, the two helium particles, ^{4}He, fused and then ^{8}Be resonant is formed ($\alpha + \alpha \rightarrow$ Be). Secondly, this ^{8}Be combined with another ^{4}He (α) particle again and ^{12}C is obtained (Be$+\alpha \rightarrow$ C*), where Be and C* denote the ^{8}Be ground state and Hoyle state of ^{12}C, respectively [47]. In our calculation, we consider the Coulomb screening effect in weakly coupled-thermal plasma. Therefore, we apply the Debye-Hückel approximation to account the Coulomb screening. The Debye screening results in the Yukawa form of the Coulomb interaction among α particles, which in turn acts to enhance carbon production [48]. For typical conditions considered here, the thermal kinetic energy of α particles is much larger than the Coulomb energy at interparticle spacing. And this is in turn dominant over the strong force two-body potential and three-body potential , $V_{ij}^{2\alpha}$ and $V_{123}^{3\alpha}$, at the same spacing.

There are two ways to evaluate such enhancement in the carbon production. The first one is called a direct one. In this direct one, the difference in the Q value between the screened and non-screened cases is obtained from the Coulomb energy of the point-like Hoyle state and then is incorporated into the Saha prediction of the carbon production dominated by the Boltzmann factor e^{Q/k_BT} [47]. Another is an indirect one. In this indirect one, the Coulomb correction to the chemical potential of each component is regarded as a point particle even for a nucleus in the Hoyle state. And this Coulomb correction is calculated in the Debye-Hückel approximation and then is incorporated into

the chemical equilibrium condition between three α particles and a nucleus in the Hoyle state [48, 49]. Both approaches must give a consistent result for the enhancement in the carbon production when our three-α system is sufficiently hot to become a weakly coupled non-degenerate plasma that is charge neutral. Here, we note that the corrections due to the electron Fermi degeneracy and/or the strong Coulomb coupling would make the α-α Coulomb interaction deviate from the simple Debye-screened form [50].

For the first approach, we need to give the C value appropriately. In the case of the Debye screening, $\lambda_D(C^{-1})$ is the Debye screening length defined as

$$\lambda_D = \left[\frac{k_B\, T}{4\pi e^2(n_e + \sum_i\ n_i Z_i^2)}\right]^{1/2}, \tag{2.13}$$

where n_i and Z_i are the averaged number density and charge number of ions of species i, and n_e is the averaged number density of electrons. Due to charge neutrality, $n_e = \sum_i Z_i n_i$ is satisfied. By assuming that hydrogen is exhausted and that $\sum_i n_i Z_i^2$ is dominated by α particles ($i = \alpha$), the value of λ_D can be estimated. The latter assumption is validated if one notes the fact that under chemical equilibrium, n_{C^*} is proportional to e^{Q/k_BT}, which is generally negligible. The value of λ_D is of the order of 10^3–10^4 fm in the range of T and ρ as considered here.

Eventually, this Debye screening length, λ_D, determines the Coulomb corrections of three α particles as

$$\Delta V_C = \sum_{j<k} \frac{4e^2}{r_{jk}} e^{-r_{jk}/\lambda_D} - \sum_{j<k}\ \frac{4e^2}{r_{jk}}, \tag{2.14}$$

where r_{jk} is the distance operator between the jth and kth α particles. The expectation value of ΔV_C can be obtained in the present three-body calculations as $\Delta E_C\ = \langle \Delta V_C \rangle$. This ΔV_C value gives rise to a decrease in the mass of the Hoyle state and hence an increase in the Q value. We have already known that the distance between the fusion particles is generally far shorter than λ_D. So, we obtain ΔE_C by using the Taylor expansion with respect to $\langle r_{jk} \rangle$.

$$\Delta E_C = -\frac{12e^2}{\lambda_D} + O\left(\langle r_{jk} \rangle\right). \tag{2.15}$$

Equation.2.15 explains that the increase in the Q value amounts to $\frac{12e^2}{\lambda_D}$ in the weak screening limit and in the zero-size limit of the Hoyle state. In our calculation, we consider that the number of electrons remains unchanged by the triple-alpha reaction. And we do not consider the gamma decay of the Hoyle state (two-photon processes) here because the lower-lying carbon states are not always described in terms of three α particles.

For the second approach, we first write down the Helmholtz free energy density of the system as

$$f\ = f_0 + f_{\rm DH}, \tag{2.16}$$

where

$$
\begin{aligned}
f_0 &= n_e m_e c^2 + \sum_i n_i m_i c^2 \\
&\quad - n_e k_B T \left\{ \ln \left[\frac{2}{n_e} \left(\frac{m_e k_B T}{2\pi\hbar^2} \right)^{3/2} \right] + 1 \right\} \\
&\quad - \sum_i n_i k_B T \left\{ \ln \left[\frac{g_i}{n_i} \left(\frac{m_i k_B T}{2\pi\hbar^2} \right)^{3/2} \right] + 1 \right\},
\end{aligned} \tag{2.17}
$$

with the electron (i ion) rest mass m_e (m_i) and the number of internal degrees of freedom of i ions g_i, is the ideal gas part of the free energy density, and

$$
f_{\rm DH} = -(n_e + \sum_i n_i Z_i^2) \frac{e^2}{3\lambda_D} \tag{2.18}
$$

is the lowest-order Coulomb correction to f_0, i.e., the Debye-Hückel term appropriate for a multi-component classical plasma. From this free energy density, one can derive the chemical potential of electrons and of i ions.

Firstly, we will derive the chemical potential of electrons. So, the Helmholtz free energy density of the electrons is

$$
\begin{aligned}
f_e &= n_e m_e c^2 - n_e k_B T \left\{ \ln \left[\frac{2}{n_e} \left(\frac{m_e k_B T}{2\pi\hbar^2} \right)^{3/2} \right] + 1 \right\} - n_e \frac{e^2}{3\lambda_D} \\
&= n_e m_e c^2 - n_e k_B T \ln \left[\frac{2}{n_e} \left(\frac{m_e k_B T}{2\pi\hbar^2} \right)^{3/2} \right] - n_e k_B T - n_e \frac{e^2}{3\lambda_D}
\end{aligned} \tag{2.19}
$$

The chemical potential for electrons is obtained as

$$
\begin{aligned}
\mu_e &= \frac{df_e}{dn_e} \\
&= m_e c^2 - \frac{d}{dn_e} \left\{ n_e k_B T \ln \left[\frac{2}{n_e} \left(\frac{m_e k_B T}{2\pi\hbar^2} \right)^{3/2} \right] \right\} - k_B T - \frac{d}{dn_e} \left\{ n_e \frac{e^2}{3\lambda_D} \right\}
\end{aligned} \tag{2.20}
$$

We will derive the second term of the right hand side of Eq.2.20.

$$
\begin{aligned}
\frac{d}{dn_e} \left\{ n_e k_B T \ln \left[\frac{2}{n_e} \left(\frac{m_e k_B T}{2\pi\hbar^2} \right)^{3/2} \right] \right\} &= k_B T \frac{d}{dn_e} \left\{ n_e \ln \left[2 \left(\frac{m_e k_B T}{2\pi\hbar^2} \right)^{3/2} n_e^{-1} \right] \right\} \\
&= k_B T \left\{ \ln \left[\frac{2}{n_e} \left(\frac{m_e k_B T}{2\pi\hbar^2} \right)^{3/2} \right] \right. \\
&\quad \left. + n_e \frac{d}{dn_e} \ln \left[2 \left(\frac{m_e k_B T}{2\pi\hbar^2} \right)^{3/2} n_e^{-1} \right] \right\}
\end{aligned} \tag{2.21}
$$

And $\ln(x^{-1}) = -\ln(x)$, so the above Eq.2.21 becomes

$$\frac{d}{dn_e}\left\{n_e k_B T \ln\left[\frac{2}{n_e}\left(\frac{m_e k_B T}{2\pi\hbar^2}\right)^{3/2}\right]\right\} = k_B T \ln\left[\frac{2}{n_e}\left(\frac{m_e k_B T}{2\pi\hbar^2}\right)^{3/2}\right] - k_B T n_e \frac{d}{dn_e}\ln\left[2\left(\frac{m_e k_B T}{2\pi\hbar^2}\right)^{3/2} n_e\right]$$

We also apply $\frac{d}{dx}\ln(x) = \frac{1}{x}$ and we get

$$\frac{d}{dn_e}\left\{n_e k_B T \ln\left[\frac{2}{n_e}\left(\frac{m_e k_B T}{2\pi\hbar^2}\right)^{3/2}\right]\right\} = k_B T \ln\left[\frac{2}{n_e}\left(\frac{m_e k_B T}{2\pi\hbar^2}\right)^{3/2}\right] - k_B T \tag{2.22}$$

Then we solve the final term of the right hand side of the Eq.2.20.

$$\frac{d}{dn_e}\left(n_e \frac{e^2}{3\lambda_D}\right) = \frac{e^2}{3}\frac{d}{dn_e}\left(n_e \lambda_D^{-1}\right) \tag{2.23}$$

λ_D for the electrons is assumed as

$$\lambda_D = \left(\frac{k_B T}{4\pi e^2 n_e}\right)^{1/2}$$

and

$$\lambda_D^{-1} = \left(\frac{k_B T}{4\pi e^2}\right)^{-1/2} n_e^{1/2}$$

Therefore, the Eq.2.23 becomes

$$\begin{aligned}
\frac{d}{dn_e}\left(n_e \frac{e^2}{3\lambda_D}\right) &= \frac{e^2}{3}\frac{d}{dn_e}\left(n_e \left(\frac{k_B T}{4\pi e^2}\right)^{-1/2} n_e^{1/2}\right) \\
&= \frac{e^2}{3}\left(\frac{k_B T}{4\pi e^2}\right)^{-1/2} \frac{d}{dn_e} n_e^{3/2} \\
&= \frac{e^2}{3}\left(\frac{k_B T}{4\pi e^2}\right)^{-1/2} \frac{3}{2} n_e^{1/2} \\
&= \frac{3e^2}{6}\left(\frac{k_B T}{4\pi e^2}\right)^{-1/2} n_e^{1/2} \\
&= \frac{e^2}{2\lambda_D}
\end{aligned} \tag{2.24}$$

We insert Eqs.2.22 and 2.24 into Eq.2.20.

$$\mu_e = m_e c^2 - k_B T \ln\left[\frac{2}{n_e}\left(\frac{m_e k_B T}{2\pi\hbar^2}\right)^{3/2}\right] + k_B T - k_B T - \frac{e^2}{2\lambda_D}.$$

Finally, the chemical potential for electrons is obtained as

$$\mu_e = m_e c^2 - k_B T \ln\left[\frac{2}{n_e}\left(\frac{m_e k_B T}{2\pi\hbar^2}\right)^{3/2}\right] - \frac{e^2}{2\lambda_D}. \tag{2.25}$$

Now, we will derive the chemical potential for i ions. The Helmholtz free energy density of the i ions can be written as

$$f_i = \sum_i n_i m_i c^2 - \sum_i n_i k_B T \left\{ \ln \left[\frac{g_i}{n_i} \left(\frac{m_i k_B T}{2\pi\hbar^2} \right)^{3/2} \right] + 1 \right\} - \sum_i n_i Z_i^2 \frac{e^2}{3\lambda_D}.$$

The chemical potential of the i ions can be obtained from the derivative of the Helmholtz free energy density.

$$\begin{aligned} \mu_i &= \frac{df_i}{dn_i} \\ &= m_i c^2 - k_B T \frac{d}{dn_i} \left\{ n_i \ln \left[\frac{g_i}{n_i} \left(\frac{m_i k_B T}{2\pi\hbar^2} \right)^{3/2} \right] \right\} \\ &\quad - k_B T - \frac{d}{dn_i} \left\{ Z_i^2 \frac{e^2}{3} n_i \lambda_D^{-1} \right\}. \end{aligned} \tag{2.26}$$

Similarly, we will solve the second term of the right hand side of the Eq.2.26.

$$k_B T \frac{d}{dn_i} \left\{ n_i \ln \left[\frac{g_i}{n_i} \left(\frac{m_i k_B T}{2\pi\hbar^2} \right)^{3/2} \right] \right\} = k_B T \ln \left[\frac{g_i}{n_i} \left(\frac{m_i k_B T}{2\pi\hbar^2} \right)^{3/2} \right] - k_B T \tag{2.27}$$

We will solve the last term of the right hand side of the Eq.2.26.

$$\frac{d}{dn_i} \left\{ Z_i^2 \frac{e^2}{3} n_i \lambda_D^{-1} \right\} = Z_i^2 \frac{e^2}{3} \frac{d}{dn_i} \left\{ n_i \, \lambda_D^{-1} \right\}. \tag{2.28}$$

For i ions, λ_D is

$$\lambda_D = \left(\frac{k_B T}{4\pi e^2 n_i Z_i^2} \right)^{1/2}$$

and

$$\lambda_D^{-1} = \left(\frac{k_B T}{4\pi e^2 Z_i^2} \right)^{-1/2} n_i^{1/2}.$$

Therefore, the Eq.2.28 becomes

$$\begin{aligned} \frac{d}{dn_i} \left\{ Z_i^2 \frac{e^2}{3} n_i \lambda_D^{-1} \right\} &= Z_i^2 \frac{e^2}{3} \frac{d}{dn_i} \left\{ n_i n_i^{1/2} \left(\frac{k_B T}{4\pi e^2 Z_i^2} \right)^{-1/2} \right\} \\ &= Z_i^2 \frac{e^2}{3} \frac{3}{2} \left(\frac{k_B T}{4\pi e^2 Z_i^2} \right)^{-1/2} n_i^{1/2} \\ &= \frac{Z_i^2 e^2}{2\lambda_D} \end{aligned} \tag{2.29}$$

We will use Eqs.2.27 and 2.29. So the Eq.2.26 becomes

$$\mu_i = m_i c^2 - k_B T \ln\left[\frac{g_i}{n_i}\left(\frac{m_i k_B T}{2\pi\hbar^2}\right)^{3/2}\right] + k_B T - k_B T - \frac{Z_i^2 e^2}{2\lambda_D}$$

Therefore, the chemical potential of the i ions is

$$\mu_i = m_i c^2 - k_B T \ln\left[\frac{g_i}{n_i}\left(\frac{m_i k_B T}{2\pi\hbar^2}\right)^{3/2}\right] - \frac{Z_i^2 e^2}{2\lambda_D} \tag{2.30}$$

The last term on the right-hand side of Eq.2.30 corresponds to the Coulomb correction, μ_i^{Coul}, to the chemical potential of i ions.

We then apply the chemical potentials given by Eqs.2.25 and 2.30 to the chemical equilibrium condition for $3\alpha \leftrightarrow \mathrm{C}^*$.

$$3\mu_\alpha = \mu_{\mathrm{C}^*}. \tag{2.31}$$

Note that μ_e does not come in because the triple-alpha process involves no beta process. If we consider the i ions are α particles, μ_i becomes

$$\mu_\alpha = m_\alpha c^2 - k_B T \ln\left[\frac{g_\alpha}{n_\alpha}\left(\frac{m_\alpha k_B T}{2\pi\hbar^2}\right)^{3/2}\right] - \frac{Z_\alpha^2 e^2}{2\lambda_D} \tag{2.32}$$

If i ions are C^* (Hoyle state of ^{12}C),

$$\mu_{\mathrm{C}^*} = m_{\mathrm{C}^*} c^2 - k_B T \ln\left[\frac{g_{\mathrm{C}^*}}{n_{\mathrm{C}^*}}\left(\frac{m_{\mathrm{C}^*} k_B T}{2\pi\hbar^2}\right)^{3/2}\right] - \frac{Z_{\mathrm{C}^*}^2 e^2}{2\lambda_D} \tag{2.33}$$

And then we use the Eqs.2.32 and 2.33 with the chemical equilibrium condition, $3\alpha \leftrightarrow \mathrm{C}^*$. So we get

$$\begin{aligned} 3m_\alpha c^2 - 3k_B T \ln\left(\frac{g_\alpha}{n_\alpha}\left(\frac{m_\alpha k_B T}{2\pi\hbar^2}\right)^{3/2}\right) - \frac{3Z_\alpha^2 e^2}{2\lambda_D} =& m_{C^*} c^2 - k_B T \ln\left(\frac{g_{\mathrm{C}^*}}{n_{\mathrm{C}^*}}\left(\frac{m_{\mathrm{C}^*} k_B T}{2\pi\hbar^2}\right)^{3/2}\right) \\ & - \frac{Z_{\mathrm{C}^*}^2 e^2}{2\lambda_D} \end{aligned} \tag{2.34}$$

$$\begin{aligned} \left(3m_\alpha - m_{\mathrm{C}^*}\right) c^2 - \frac{3Z_\alpha^2 e^2}{2\lambda_D} + \frac{Z_{\mathrm{C}^*}^2 e^2}{2\lambda_D} =& 3k_B T \ln\left(\frac{g_\alpha}{n_\alpha}\left(\frac{m_\alpha k_B T}{2\pi\hbar^2}\right)^{3/2}\right) \\ & - k_B T \ln\left(\frac{g_{C^*}}{n_{\mathrm{C}^*}}\left(\frac{m_{\mathrm{C}^*} k_B T}{2\pi\hbar^2}\right)^{3/2}\right) \end{aligned} \tag{2.35}$$

And we use $Z_\alpha = 2$ and $Z_{\mathrm{C}^*} = 6$.

$$\begin{aligned}
\left(3m_\alpha - m_{\mathrm{C}^*}\right)c^2 - \frac{32^2e^2}{2\lambda_D} + \frac{6^2e^2}{2\lambda_D} =& 3k_BT\ln\left(\frac{g_\alpha}{n_\alpha}\left(\frac{m_\alpha k_BT}{2\pi\hbar^2}\right)^{3/2}\right) \\
& - k_BT\ln\left(\frac{g_{\mathrm{C}^*}}{n_{\mathrm{C}^*}}\left(\frac{m_{\mathrm{C}^*}k_BT}{2\pi\hbar^2}\right)^{3/2}\right) \\
\left(3m_\alpha - m_{\mathrm{C}^*}\right)c^2 - \frac{12e^2}{2\lambda_D} =& k_BT\ln\left(\frac{g_\alpha^3}{n_\alpha^3}\left(\frac{\sqrt{m_\alpha k_BT}}{\sqrt{2\pi}\hbar}\right)^9\right) \\
& - k_B\,T\ln\left(\frac{g_{\mathrm{C}^*}}{n_{\mathrm{C}^*}}\left(\frac{m_{\mathrm{C}^*}k_BT}{2\pi\hbar^2}\right)^{3/2}\right) \qquad (2.36)
\end{aligned}$$

We assume that $Q_0 = (3m_\alpha - m_{\mathrm{C}^*})c^2$ is the Q value in the ideal gas limit, $\lambda_i = \sqrt{2\pi}\hbar/\sqrt{m_i k_BT}$ is the thermal de Broglie wavelength, and $g_{\mathrm{C}^*} = g_\alpha = 1$. So, the Eq.2.36 becomes

$$\begin{aligned}
Q_0 + \frac{12e^2}{\lambda_D} &= k_BT\Big\{\ln\left(\frac{1}{n_\alpha^3}\frac{1}{\lambda_\alpha^9}\right) - \ln\left(\frac{1}{n_{\mathrm{C}^*}}\frac{1}{\lambda_{\mathrm{C}^*}^3}\right)\Big\} \\
\frac{Q_0}{k_BT} + \frac{12e^2}{\lambda_D k_BT} &= \ln\left(\frac{n_{\mathrm{C}^*}\lambda_{\mathrm{C}^*}^3}{n_\alpha^3\lambda_\alpha^9}\right) \\
e^{\left(\frac{Q_0}{k_BT} + \frac{12e^2}{\lambda_D k_BT}\right)} &= \frac{n_{C^*}\lambda_{\mathrm{C}^*}^3}{n_\alpha^3\lambda_\alpha^9} \qquad (2.37)
\end{aligned}$$

Finally, we obtain

$$n_{\mathrm{C}^*} = n_\alpha^3 e^{Q_0/k_BT}\lambda_\alpha^9\lambda_{\mathrm{C}^*}^{-3}e^{12e^2/\lambda_D k_BT}, \qquad (2.38)$$

In the absence of screening, Eq.2.38 reduces to the Saha prediction of the carbon production. The Debye screening induces the factor $e^{12e^2/\lambda_D k_BT}$ via $3\mu_\alpha^{\mathrm{Coul}}\mu_{C^*}^{\mathrm{Coul}} = 12e^2/\lambda_D$, which is consistent with the first approach that predicts an increase in the Q value by $12e^2/\lambda_D$ in the weak screening limit.

2.2 Three-α description of the Hoyle state

In this section, we describe how to obtain the three-α wave function.

2.2.1 Variational Principle

The variational method is one way to approximate the lowest energy eigenstate or ground state as well as some excited states. This allows calculating the approximate wave functions. The basis for this method is the variational principle (or) Ritz theorem. So, We will briefly explain the variational principle.

Consider the ground state of some arbitrary system. The ground state wave function ψ_0 and E_0 satisfy the Schrödinger equation

$$\hat{H}\psi_0 = E_0\psi_0. \tag{2.39}$$

For an arbitrary function ψ of the state space, the expectation value (mean value) of H in the state ψ is such that

$$\langle E\rangle = \frac{\langle\psi|\hat{H}|\psi\rangle}{\langle\psi|\psi\rangle} \geq E_0. \tag{2.40}$$

Any approximation to the ground state wave function will yield an expectation value of the Hamiltonian that is greater than or equal to the ground state energy. Equality is satisfied only in the case that the approximate wave function is also a ground state wave function.

By modifying ψ as $\psi + \delta\psi$ and by omitting the higher order terms, the energy expectation value becomes

$$\begin{aligned}\langle\psi|\psi\rangle\delta E + E\delta\left(\langle\psi|\psi\rangle\right) &= \langle\psi|H|\delta\psi\rangle + \langle\delta\psi|H|\psi\rangle \\ \langle\psi|\psi\rangle\delta E &= \delta\left(\langle\psi|H|\psi\rangle\right) - E\delta\left(\langle\psi|\psi\rangle\right) \\ &= \langle\delta\psi|H-E|\psi\rangle + \angle\psi|H-E|\delta\psi\rangle. \end{aligned} \tag{2.41}$$

If $\delta E = 0$ for any infinitesimal $\delta\psi$, the mean value E becomes stationary. Therefore, $\langle\delta\psi|H-E|\psi\rangle + \langle\psi|H-E|\delta\psi\rangle = 0$.

If $\delta\psi$ is chosen to be $\epsilon(H-E)\psi$, where ϵ is an infinitesimal real number, the above equation implies that the norm of the function $(H-E)\psi$ is zero and thus the function $(H-E)\psi$ itself must be a null function, namely $H\psi = E\psi$. Therefore the mean value E is stationary if and only if the state ψ from which E is calculated is an eigenstate of H, and the stationary value E is the corresponding eigenvalue of the Hamiltonian. If the guess is not exactly the right ground state wave function then it can be expressed as the linear combination of complete set of Hamiltonian eigenstates. So, the linear combination of a finite number of independent functions $\psi(\alpha)$ can be expressed as

$$\psi = \sum_{n=1}^{K} c_i\psi(\alpha_i). \tag{2.42}$$

Here, c_i is an expansion coefficient and $\psi(\alpha_i)$ is the trial wave function. The expectation value E is given by

$$E = \frac{c^\dagger Hc}{c^\dagger Bc}, \tag{2.43}$$

where, c is a K-dimensional column vector whose ith element is c_i and $c^\dagger$ is the Hermitian conjugate of c.
The $K \times K$ Hamiltonian and overlap matrices H and B are defined by

$$H_{ij} = \langle\psi(\alpha_i)|H|\psi(\alpha_j)\rangle \qquad , B_{ij} = \langle\psi(\alpha_i)|\psi(\alpha_j)\rangle. \tag{2.44}$$

The linear parameter c_i can be determined by the generalized Ritz theorem. The condition that E is stationary with respect to an arbitrary, infinitesimal change of c_i leads to the generalized problem.

$$Hc = EBc \qquad , i.e., \qquad \sum_{j=1}^{K}(H_{ij} - EB_{ij})c_j = 0 \qquad (i = 1, ..., K) \tag{2.45}$$

We therefore have i simultaneous secular equations in i unknowns. These equations can also be written in matrix notation, and for a non-trivial solution (i.e. $c_i \neq 0$ for all i), the determinant of the secular matrix must be equal to zero i.e. $|H_{ij} - EB_{ij}| = 0$. The resulting algebraic equation can be solved to obtain the energies E.

2.2.2 Variational calculation with correlated Gaussian expansion

We will start by summarizing a variational approach that will be used to obtain a precise solution of the three-body Schrödinger equation.

For the three-α system, the Hamiltonian is written as

$$H = \sum_{i=1}^{3} T_i - T_{\rm cm} + \sum_{i<j} \left[V_{ij}^{2\alpha} + V_{ij}^{\rm Coul} \right] + V_{123}^{3\alpha}, \tag{2.46}$$

where, T_i is the kinetic energy operator of the ith α particle, and the center-of-mass kinetic energy $T_{\rm cm}$ is appropriately subtracted. Detail explanation of the two-and three-α potentials, $V_{ij}^{2\alpha}$ and $V_{123}^{3\alpha}$, as well as the Coulomb potential $V_{ij}^{\rm Coul}$, will be given in the next section.

The wave function of the three-α system can be expanded by a number (K) of symmetrized ($\mathcal{S}$) correlated Gaussian basis function G as

$$\Psi^{(n)} = \sum_{k=1}^{K} c_k^{(n)} \mathcal{S}G(A_k, \boldsymbol{x}). \tag{2.47}$$

The set of coefficients $(c_1(n), ..., c_K(n))$, where n denotes a label of the state ($n = 0, ..., K-1$) with $n = 0$ being the ground state, can be determined by solving the generalized eigenvalue equation

$$\sum_{j=1}^{K} H_{ij} c_j^{(n)} = E^{(n)} \sum_{j=1}^{K} B_{ij} c_j^{(n)}, \tag{2.48}$$

where

$$\begin{aligned} H_{ij} &= \langle \mathcal{S}G(A_i, \boldsymbol{x}) | H | \mathcal{S}G(A_j, \boldsymbol{x}) \rangle \\ B_{ij} &= \langle \mathcal{S}G(A_i, \boldsymbol{x}) | \mathcal{S}G(A_j, \boldsymbol{x}) \rangle \end{aligned} \tag{2.49}$$

are the Hamiltonian and overlap matrix elements, respectively.

Here, the coordinate set $\tilde{\boldsymbol{x}} = (\boldsymbol{x}_1, \boldsymbol{x}_2)$, where the tilde denotes the transpose of the matrix, is taken as the Jacobi coordinates excluding the center of mass of the three-α system $\boldsymbol{x}_3$. These three coordinates are defined as

$$\boldsymbol{x}_i = \sum_{j=1}^{3} U_{ij}\, \boldsymbol{r}_j \qquad\qquad (i = 1, 2, 3), \tag{2.50}$$

where, $\boldsymbol{r}_j$ denotes the jth single-α coordinate, and

$$U = \begin{pmatrix} 1 & -1 & 0 \\ \frac{1}{2} & \frac{1}{2} & -1 \\ \frac{1}{3} & \frac{1}{3} & \frac{1}{3} \end{pmatrix} \tag{2.51}$$

is the transformation matrix of the 3-α system.

Finally, the correlated Gaussian basis function is defined by [30, 31]

$$\begin{aligned} G(A,\boldsymbol{x}) &= \exp\left(-\frac{1}{2}\tilde{\boldsymbol{x}}A_{ij}\boldsymbol{x}\right) \\ &= \exp\left(-\frac{1}{2}A_{11}x_1^2 - \frac{1}{2}A_{22}x_2^2 - A_{12}\boldsymbol{x}_1\cdot\boldsymbol{x}_2\right) \end{aligned} \tag{2.52}$$

A symmetric, positive-definite 2×2 matrix A defines each correlated Gaussian. The Gaussian falloff parameters are related to the diagonal elements of the matrix A as $1/\sqrt{A_{ii}}$, while the off-diagonal element controls the correlations among the different relative coordinates. Because of analytical form of matrix elements, the correlated Gaussians have an significant advantage. These matrix elements can be calculated very accurately and fast. Another major advantage of correlated Gaussian is that the interparticle interaction can be treated with equal prominence for all pairs of particles. This makes the correlated Gaussian basis sets suitable for treating systems with attractive interactions that result in strong interparticle correlations.

Under the interchange of identical particles, the wave function of the system must have a proper symmetry. The symbol $\mathcal{S}$ stands for a symmetrizer, which ensures that the basis function is completely symmetric with regard to any exchange of particles. One of the key advantages of the correlated Gaussian is that its functional form is invariant under any coordinate transformation, allowing us to easily manipulate exchanges of the particles as needed for the symmetrization of the basis function.

The symmetrizer $\mathcal{S}$ is defined as $S = (1/\sqrt{(3!)})\sum_P P$. The permutation

$$P = \begin{pmatrix} 1 & 2 & 3 \\ p_1 & p_2 & p_3 \end{pmatrix}$$

of particle indices transforms the single-particle coordinate as $\boldsymbol{r}_i \to \boldsymbol{r}_{p_i}$:

$$P\boldsymbol{r} = T_P\boldsymbol{r}, \tag{2.53}$$

where, the matrix T_P is

$$(T_P)_{ij} = \delta_{jP_i} \qquad (i,j = 1,...,3). \tag{2.54}$$

So, we superpose the six permutations among the three identical bosons, which may then be described using an appropriate choice of the transformation matrix T_P. The matrices T_P are given as follows in the case of three-α particles:

$$T\left(\begin{smallmatrix}1&2&3\\1&2&3\end{smallmatrix}\right) = \begin{pmatrix} 1 & 0 & 0 \\ 0 & 1 & 0 \\ 0 & 0 & 1 \end{pmatrix}, \quad T\left(\begin{smallmatrix}1&2&3\\2&1&3\end{smallmatrix}\right) = \begin{pmatrix} 0 & 1 & 0 \\ 1 & 0 & 0 \\ 0 & 0 & 1 \end{pmatrix},$$

$$T\left(\begin{smallmatrix}1&2&3\\3&2&1\end{smallmatrix}\right)=\begin{pmatrix}0&0&1\\0&1&0\\1&0&0\end{pmatrix}\quad,\quad T\left(\begin{smallmatrix}1&2&3\\1&3&2\end{smallmatrix}\right)=\begin{pmatrix}1&0&0\\0&0&1\\0&1&0\end{pmatrix},$$

$$T\left(\begin{smallmatrix}1&2&3\\2&3&1\end{smallmatrix}\right)=\begin{pmatrix}0&1&0\\0&0&1\\1&0&0\end{pmatrix}\quad,\quad T\left(\begin{smallmatrix}1&2&3\\3&1&2\end{smallmatrix}\right)=\begin{pmatrix}0&0&1\\1&0&0\\0&1&0\end{pmatrix}.$$

When the wave function is defined in terms of the relative coordinates, the permutation P induces a linear transformation of the relative coordinates as follows:

$$P\boldsymbol{x}=T_P\boldsymbol{x} \tag{2.55}$$

where, $(T_P)_{ij}=\sum_{k=1}^{3}U_{ik}(U^{-1})_{p_kj}\qquad(i,j=1,2)$.
The permutation P acts on the correlated Gaussian as

$$PG(A,\boldsymbol{x})=G(\tilde{P}AP,\boldsymbol{x}). \tag{2.56}$$

Therefore, the symmetrization requirement on the trial function amounts to a simple multiplication of the matrix $\tilde{P}AP$. This convenient property makes the correlated Gaussian basis suitable for treating few-body systems accompanied by strong interparticle correlations [35, 36].

The majority of the matrix elements, including H_{ij} and B_{ij}, can be calculated analytically as functions of a set of variational parameters, i.e., the matrix elements A_{ij} for each basis [30, 31, 37], which are then optimized using the stochastic variational method [30, 31]. In practice,the diagonal matrix elements of the matrix A are generated as random numbers in the ranges of $0<1/\sqrt{A_{11}}<20$ fm and $0<2/\sqrt{3A_{22}}<20$ fm so that the asymptotic wave function due to the Coulomb screening may be described at large distances. The correlation among the particles is taken into account via the off-diagonal matrix element A_{12}, which is determined by defining the 2D rotation matrix $R(\theta)$ with randomly generated rotational angles θ and multiplying it by the diagonal matrix $D_{ij}=A_{ij}\delta_{ij}$ as $\tilde{R}DR$.

2.2.3 Potential terms in the three-α Hamiltonian

An effective potential between the α particles was studied phenomenologically or by a resonating group method (RGM). In our calculation, we use the phenomenological potential. For describing the two-body interaction $V_{ij}^{2\alpha}$ in Eq.2.46, we use the modified Ali-Bodmer (AB) potential [38, 41]. The two-body modified Ali-Bodmer (AB) potential is given by

$$V_{ij}^{2\alpha} = v_r \exp\left(-\frac{r_{ij}^2}{b_r^2}\right) - v_a \exp\left(-\frac{r_{ij}^2}{b_a^2}\right), \tag{2.57}$$

where $v_r = 125$ MeV, $b_r = 1.53$ fm and $v_a = 30.18$ MeV , $b_a = 2.85$ fm. Energy and length are given in units of MeV and fm, respectively. The original Ali-Bodmer potential is l dependent. But we ignore the l dependence and we use only the S-wave potential for all partial waves.

The Coulomb potential is expressed as

$$V_{ij}^{\mathrm{Coul}} = \frac{4e^2}{r_{ij}}. \tag{2.58}$$

In this work, the mass m of the α particle is defined as $\hbar^2/m = 10.5254$ MeV fm^2 and the charge constant is $e^2 = 1.4399644$ MeV fm.

Finally, we will consider the three-α potential $V_{123}^{3\alpha}$. We use the three-α potential $V_{123}^{3\alpha}$ from Ref. [15]. The $V_{123}^{3\alpha}$ is

$$V(ij) = -5.33 \exp\left(-\frac{r_{ij}^2}{2.58^2}\right). \tag{2.59}$$

By applying these potentials, we calculated the ground state and Hoyle state of the three-α system. And then we compared our results with Ref. [15]. After calculating the energy values of the three-α particles, we calculated the energies of the Hoyle state with the Coulomb screening effect. Next section, we will explain the potential terms in the three-α Hamiltonian with the Coulomb screening factor.

2.2.4 Potential terms in the three-α Hamiltonian with Coulomb screening factor

We assume the α particle is an inert point boson to describe $V_{ij}^{2\alpha}$ in Eq.2.46 not only in a simple form but also to reasonably reproduce low-energy α-α scattering data. There are several versions of the potential models that can be constructed under such an assumption (see,e.g., Refs. [38, 39, 40]). The modified Ali-Bodmer (AB) potential [38, 41] is used in this study, and it is designed to provide the S-wave ^{8}Be (0_1^+) resonance position E_r with 88.84 keV [15], which is near to the empirical value of 91.8 keV [42]. The explicit form of the potential is given by

$$V_{ij}^{2\alpha} = v_r \exp\left(-\frac{r_{ij}^2}{b_r^2}\right) - v_a \exp\left(-\frac{r_{ij}^2}{b_a^2}\right), \tag{2.60}$$

where $v_r = 125$ MeV, $b_r = 1.53$ fm and $v_a = 30.18$ MeV , $b_a = 2.85$ fm. And the energy and length are given in units of MeV and fm, respectively, and $r_{ij} \equiv |\boldsymbol{r}_i - \boldsymbol{r}_j|$.

To account for the Debye screening in thermal plasmas, we use the Yukawa form to substitute the bare Coulomb potential between point charges located at $\boldsymbol{r}_i$ and $\boldsymbol{r}_j$:

$$V_{ij}^{\rm Coul} = \frac{4e^2}{r_{ij}} \exp\left(-C r_{ij}\right). \tag{2.61}$$

The parameter C represents the inverse of the length of the Coulomb screening. We mention in passing that the charge form factor of an α particle, f, can be incorporated into Eq.2.61 for more realistic calculations:

$$\begin{aligned} V_{ij}^{\rm Coul} &= \int d^3u_i \int d^3u_j f(\boldsymbol{u}_i) f(\boldsymbol{u}_j) \frac{4e^2}{|(\boldsymbol{r}_i + \boldsymbol{u}_i) - (\boldsymbol{r}_j + \boldsymbol{u}_j)|} \\ &\quad \times \exp\left(-C|(\boldsymbol{r}_i + \boldsymbol{u}_i) - (\boldsymbol{r}_j + \boldsymbol{u}_j)|\right), \end{aligned} \tag{2.62}$$

where the integral of f over the whole space is set to unity. To include such a finite-size effect in the three-α system, it is reasonable to assume the Gaussian charge form factor for the α particle, leading to the explicit form of the Coulomb potential,

$$V_{ij}^{\rm Coul} = \frac{4e^2}{r_{ij}} {\rm erf}(\kappa r_{ij}) \exp\left(-C r_{ij}\right), \tag{2.63}$$

with $\kappa = 0.6014$ fm^{-1} [15]. We will use Eq.2.63 unless otherwise noted.

Finally, we consider the three-α potential, which occurs naturally as a result of the internal structure of each α particle. This potential must be considered because it is well known that the empirical energies of the states close to the three-α threshold are not well reproduced from the two-α potential alone [43]. As was done in Ref. [15], one can introduce a simplified potential among three point α particles in the form of

$$V_{123}^{3\alpha} = v_r \exp\left(-\frac{R^2}{b_r^2}\right) - v_a \exp\left(-\frac{R^2}{b_a^2}\right) \tag{2.64}$$

with $R^2 \equiv \sqrt{3}\sum_{i=1}^{3}(\boldsymbol{r}_i - \boldsymbol{x}_3)^2 = \frac{\sqrt{3}}{2}x_1^2 + \frac{2}{\sqrt{3}}x_2^2$. We use two types of three-α potentials to see the model dependence. One is a potential with only an attractive term [15]; the parameters are set to $v_r = 0$, $v_a = 152.2$ MeV, and $b_a = 2.58$ fm (Set 1) to reproduce the empirical Hoyle state energy in vacuum. We note that, as given in Ref. [17], not only is the experimental charge radius of the ^{12}C ground state well reproduced from this Hamiltonian, but also the calculated Hoyle state radius is consistent with other cluster model calculations as well as the results obtained by the Tohsaki-Horiuchi-Schuck-Röpke wave function [44]. The other contains a repulsive term, which reasonably occurs given the Pauli principle among three α particles composed of nucleons [45, 46]. We set the parameters as $v_r = 48.0$, $b_r = 1.20$ fm, $v_a = 134.0$ MeV, and $b_a = 2.66$ fm (Set 2), to produce a completely different version of the three-α potential while roughly keeping the reproducibility of the empirical Hoyle state energy in vacuum. We expect some difference in the spatial scale of the Hoyle state in vacuum due to the difference in the structure of these two models for the three-α potential, which may lead to a difference in the energy of the Hoyle state at nonzero C in such a way that the larger the scale, the stronger the Coulomb screening.

The physical constants that we employ in this thesis are $\hbar^2/m_\alpha = 10.5254$ MeV fm^2 and $e^2 = 1.43996$ MeV fm, where m_α is the mass of an α particle in vacuum.

Chapter 3

Results and Discussions

In this chapter, firstly we will discuss the results of three-α system. Then, we proceed to exhibit the numerical results for the energy and size of the Hoyle state in weakly coupled thermal plasmas. The former will then be compared to the previous section's point-charge prediction of the Q value shift.

3.1 Coulomb screening effects on the three-α system

The ground state of ^{12}C corresponds to the lowest-energy state ($n = 0$) in the current Hamiltonian framework (2.46), while the Hoyle state emerges as a resonant/bound excited state. Because the Hoyle state's decay width is small, such a resonant state can be regarded as a bound state [51, 52, 53]. The ground state energy of ^{8}Be in the two-α system is obtained as 88.8 keV. The energies of the ^{12}C ground state and the Hoyle state with the Set 1 Hamiltonian ($C = 0$) are -9.40 and 0.349 MeV, respectively, which are consistent with the results of Ref. [15], while the energies of the ground state and the Hoyle state with the Set 2 Hamiltonian ($C = 0$) are -8.99 and 0.475 MeV, respectively.

The energies of the screened Hoyle state and the ground state of ^{8}Be with respect to the three-α threshold, E_{C^*} and E_{Be}, are plotted as a function of the Coulomb screening factor C in the Fig. 3.1. The Hoyle state energy drops as the Coulomb screening factor C increases, eventually approaching the three-α energy calculated in the Hamiltonian without the Coulomb term. Now we will search the Efimov state for the three-alpha system. The existence of resonant two-body forces is the fundamental condition for Efimov states. A system of the three particles with resonant two-body interactions may form bound states, the so-called Efimov states or Efimov trimers. When $C = 0.0162$ fm^{-1}, $E_{\rm Be}$ becomes $\sim 10^{-5}$ MeV, indicating that the criterion for the appearance of the Efimov state has been met. Despite this, we find that the Hoyle state is still in a resonance state for both Hamiltonians with $E_{\rm C^*} = 0.082(0.210)$ MeV for Set 1 (Set 2), ruling out the possibility that the Hoyle state is bound by the Efimov attraction. Beyond $C\sim 0.05$ fm^{-1}, the Hoyle state becomes a bound state, with an energy lower than the ^{8}Be

one, and the asymptotic energy ($C = \infty$) calculated with Set 2 is -3.62 MeV, slightly higher than that calculated with Set 1 (-3.89 MeV), because Set 2 includes the repulsive component in the three-α potential. The Debye-Hückel approximation is not valid in this case because the screening is too strong. We can also see that the behavior of the energy shift at small C is unaffected by the choice of the three-α potential, which will be discussed quantitatively later in this section.

We calculate the root-mean-square (rms) pair distance defined by $d^{(n)} = \sqrt{\langle\psi^{(n)}|x_1^2|\psi^{(n)}\rangle}$ to investigate more details of the correlated motion of the three-α system. Figure. 3.2 plots the results for the rms pair distance of the Hoyle state as a function of C, together with those of the ground state of ^{8}Be for comparison. Although the wave function calculated here well reproduces the empirical energy and decay width of ^{8}Be [15], we note that a significantly large rms pair distance 6.3 fm of ^{8}Be is obtained as compared to the *ab initio* calculation 4.8 fm [54]. Due to the stronger binding in the three-α system, the rms pair distance of the Hoyle state with Set 1 Hamiltonian is much shorter than that of the ^{8}Be ground state as long as C is small. The rms pair distance of the ^{8}Be ground state coincides with that of the Hoyle state at a critical C where the Hoyle state becomes bound. Set 2, on the other hand, gives the Hoyle state with a pair distance that is longer than not just the quantity calculated from Set 1, but also the ^{8}Be result for any positive C. The repulsive component of the three-α potential in Set 2 is responsible for this behavior. In fact, at $C = \infty$, the rms pair distance of the ^{8}Be ground state becomes 4.75 fm, but the rms pair distance of C^* is 4.75 fm for Set 1 and 4.92 fm for Set 2. In the case of $C = 0 (C = \infty)$, such repulsion also increases the rms radius of the Hoyle state, which is 3.43 (2.74) fm for Set 1and 3.71 (2.84) fm for Set 2, respectively, measured from the center of mass of the system.

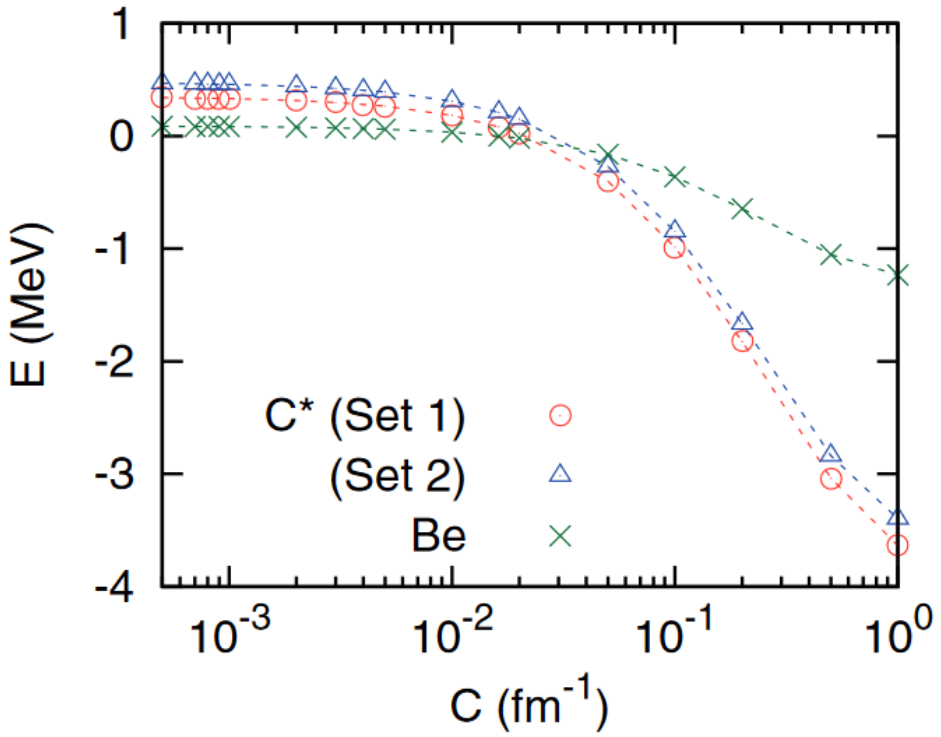

Figure 3.1: Energy of the screened Hoyle state of the three-α system calculated with respect to the three-α threshold as a function of the screening factor C. The result for the screened ground state of ^{8}Be is also plotted for comparison.

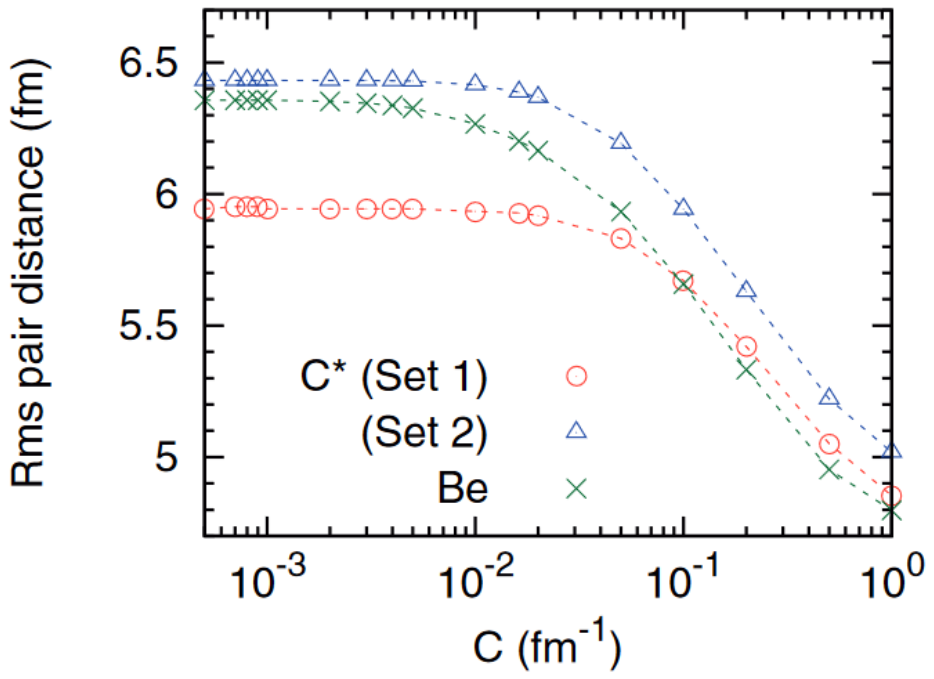

Figure 3.2: Root-mean-square (rms) pair distances of the screened Hoyle state and of the screened ^{8}Be ground state calculated as a function of the screening factor C.

3.2 Screening-induced enhancement of carbon production

Consider the case where the value of C is set to λ_D^{-1}, which is the inverse of the Debye screening length (Eq. 2.13). λ_D is useful in a plasma where all the constituents (ions and electrons) behave like a nearly ideal thermal gas. The Fermi degeneracy, for example, can play a role in modifying the current description of the screening correction to the Coulomb interaction, as proposed in Sect. 2.1.2, at the highest density of interest here.

Then, taking into account the Hoyle state's spatial structure, which was precisely evaluated in the previous subsection, we reestimate the screening-induced enhancement of carbon production in normal stars. We apply the same logic as the direct approach mentioned in Sect. 2.1.2 to do this. We simply substitute $E_{C^*}(C)$ for Q and estimate the screening-induced Q value shift and enhancement factor as $\Delta Q(C) = E_{C^*}(C=0) - E_{C^*}(C)$ and $e^{\Delta Q(C)/k_BT}$, respectively, instead of using the zero-size limit as in Sect. 2.1.2.

Finally, we compare the Q value shift owing to the screening, $\Delta Q(C)$, to the conventional prediction, $12e^2/\lambda_D$, for point charges. We present such a comparison in Fig. 3.3 by treating C as λ_D^{-1}. The three-α potential and the size of the Hoyle state do not affect the ΔQ values produced. The results for both Set 1 and Set 2 agree with the conventional prediction in the limit of $C \to 0$, as they should. Such an agreement appears to exist for typical λ_D. We also evaluate $\Delta Q(C)$ using the three-α calculations with the point-charge Coulomb potential of Eq.2.61 and find that the results are almost equivalent to those in Fig. 3.3.

Despite such a good agreement, the screening-induced Q value shift between the finite-size and zero-size cases of the Hoyle state must differ. This difference is expected to depend on the model used for the three-α potential, as explained in Sect. 2.2.4, because the two models give an appreciable difference in the prediction of the spatial scale of the Hoyle state as shown in Fig. 3.2. However, using the present $\Delta Q(C)$ results with the Yukawa form of the Coulomb potential to estimate the difference in the Q value shift, may be inappropriate because the Debye-Hückel approximation holds only for a description of the long-range Coulomb screening even in the weak coupling and classical limit. Indeed, within this approximation, the radial distribution function, $g(r)$, for α particles, i.e., the probability of finding another α particle at a distance or r from the origin at which an α particle is already located, is known to be negative near $r = 0$ and hence unphysical [55]. In the case of triple-alpha reactions, the fusing α particles are inevitably located near the partner. As a result, the short-range spatial correlation must be appropriately considered. Here we estimate such an effect on the present Q value shift. To do so, it is convenient to note that for thermal plasmas one can generally express $g(r)e^{4e^2/rk_BT}$ in a power series of r^2 near $r = 0$ [56]. Then it is reasonable to define the effective potential $w(r)$ between

two α particles via $g(r) = e^{-w(r)/k_BT}$. According to Ref. [57], $w(r)$ can be expanded as

$$w(r) = \frac{4e^2}{r} - \frac{4e^2}{\lambda_D} + \frac{1}{4}\frac{4e^2}{a_\alpha}[\frac{r}{a_\alpha}]^2 + O(r^4) \tag{3.1}$$

with $a_\alpha = (3/4\pi n_\alpha)^{1/3}$. The second term on the right-hand side corresponds to $-(2\mu_\alpha^{\rm Coul} - \mu_{\rm Be}^{\rm Coul})$, i.e., the conventional point-charge prediction of the screening-induced Q value shift for $\alpha+\alpha \rightarrow$ Be under chemical equilibrium $2\alpha \leftrightarrow$Be, while the third term comes from two closely separated α particles in the uniform electron background. For typical separation as depicted in Fig. 3.2 as well as for typical T and ρ, the ratio of the third to the second term is only of the order of 10^{-7}. The use of $w(r)$ instead of the Yukawa potential in Eq.2.14 would thus reproduce the screening-induced Q value shift of the triple-alpha process in the point-charge approximation, $12e^2/\lambda_D$, while adding an $O(10^{-7})$ correction due to the finite-size effect of the Hoyle state.

This means that the difference in such a Q value shift between the two models for the three-α potential would also be negligible. We remark in passing that in the present estimate of the terms beyond the second one in Eq.3.1, possible corrections due to the electron screening, the strong force potential $V_{ij}^{2\alpha}$, and the quantum nature of fusing α particles are ignored.

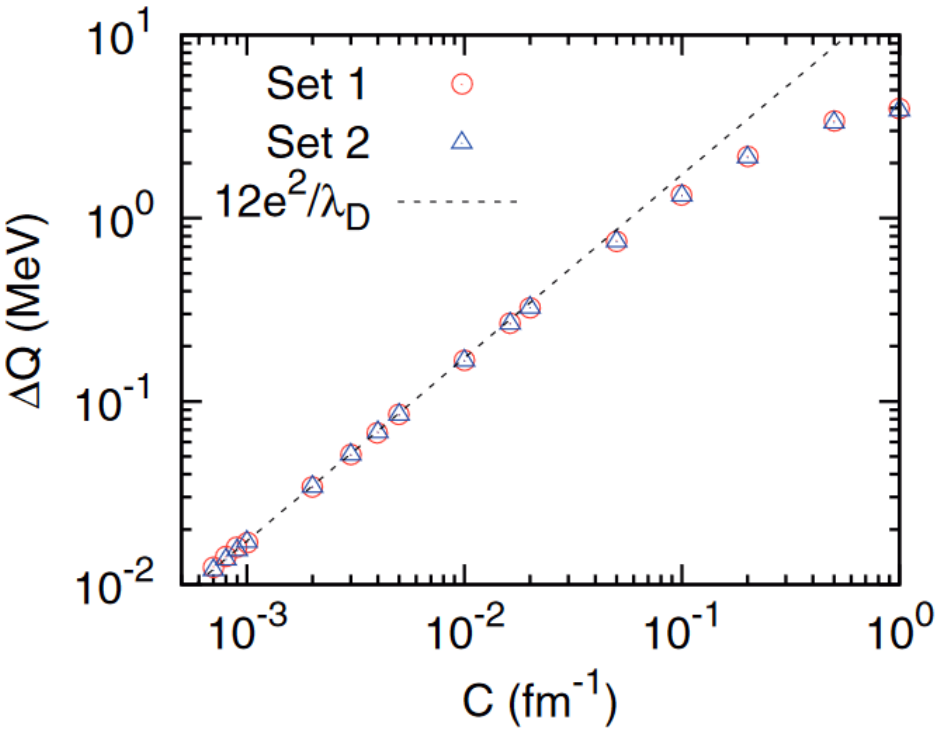

Figure 3.3: Screening-induced Q value shifts of the Hoyle state calculated as a function of C via $\Delta Q(C) = E_{C^*}(C=0) - E_{C^*}(C)$. The dashed line denotes the logarithm of the screening-induced enhancement factor with λ_D being identified with C^{-1}.

Chapter 4

Conclusion

In our thesis, we have calculated the Coulomb screening correction to the Q value of the triple-alpha process in weakly-coupled thermal plasmas. In our calculations, we employ the precise three-alpha wave function within Debye-Hückel approximation. For Coulomb screening, we use the screened Coulomb potential instead of the bare Coulomb potential. Firstly, we find that our obtained results are well in agreement with the results obtained from the conventional point-charge analysis. The conventional point-charge analysis gives a very good estimate of the screening-induced Q value shift in normal stars that undergo stable burning of helium. Finally, we also investigate the conjecture made in Ref. [32, 33] that the Hoyle state could emerge from the Efimov state. But we do not find these states with our three-body calculation within the Yukawa form of the Coulomb potential. There has recently been experimental proof that there is no Efmiov effect in ^{12}C [58]. In this paper, they did not find any evidence fot the Efimov states in ^{12}C.

Many questions nevertheless remain. It would be simple to perform the same type of three-body calculations using a more realistic situation, such as the effective Coulomb potential (Eq.3.1) rather than the Yukawa potential (Eq.2.14). In the future, we want to extend this work to explore the existence and stability of the three-alpha system in different astrophysical environments as may be encountered in X-ray bursting accreting neutron stars.

Bibliography

[1] H. Yukawa, Proc.-Math. Soc. Jpn. **17**, 48 (1935).

[2] R. D. Woods and D. S. Saxon, Phys. Rev. **95**, 577 (1954).

[3] G. Gamow, Proc. Roy. Soc. A **126**, 632 (1930).

[4] G. Gamow, *Constitution of Atomic Nuclei and Radioactivity*, (Oxford University Press,193)

[5] L. R. Hafstad, E. Teller, Phys. Rev. **54**, 681 (1938).

[6] K. Ikeda, et. al., Prog. Theor. Phys. Suppl. 464 (1968).

[7] J. A. Wheeler, Phys. Rev. **52**, 1083 (1937).

[8] K. Wildermuth and Y. C. Tang, *A Unified Theory of the Nucleus*, (Vieweg, Braunschweig, Germany, 1977)

[9] D. M. Brink, Proceedings ofthe International School of Physics "Enrico Fermi", Course **36**, 247 (1966).

[10] S. Saito., Prog. Theor. Phys. **40**, 893 (1968); **41**, 705 (1969); Prog. Theor. Phys. Suppl. **62**, II (1977).

[11] C. Beck (ed.), Clusters in Nuclei (Springer, Berlin, 2010), Vol. 1.

[12] C. Beck (ed.), Clusters in Nuclei (Springer, Berlin, 2012), Vol. 2.

[13] C. Beck (ed.), Clusters in Nuclei (Springer, Berlin, 2014), Vol. 3.

[14] S. Ishikawa, Phys. Rev. C **87**, 055804 (2013).

[15] H. Suno, Y. Suzuki, and P. Descouvemont, Phys. Rev. C **91**, 014004 (2015).

[16] T. Akahori, Y. Funaki, and K. Yabana, Phys. Rev. C **92**, 022801(R) (2015).

[17] H. Suno, Y. Suzuki, and P. Descouvemont, Phys. Rev. C **94**, 054607 (2016).

[18] E. E. Salpeter, Astrophys. J., 115, 326 (1952).

[19] H. Bethe, Phys. Rev. **55**, 434 (1939).

[20] E. Öpik, Proc. R. Ir. Acad. A **54**, 49 (1951).

[21] F. Hoyle, Astrophys. J. Suppl. Ser., **1**, 12 (1954).

[22] D. N. F. Dunbar, R. E. Pixley, W. A. Wenzel, Phys. Rev., **92**, 649 (1953).

[23] E. Epelbaum, H. Krebs, T.A. Lähde, D. Lee, Ulf-G. Meißner, Phys. Rev. Lett. **110**, 112502 (2013).

[24] Y. Funaki, H. Horiuchi, W. von Oertzen, G. Roepke, P. Schuck, A. Tohsaki, T. Yamada, Phys. Rev. C **80**, 064326 (2009).

[25] W. H. G. Lewin, J. van Paradijs, and R. E. Taam, Space Sci. Rev., **62**, 223 (1993).

[26] E.-E. Salpeter, Aust. J. Phys., **7**, 373 (1954).

[27] P. Debye and E. H́uckel, Phys. Zeitschr. **24**, 185 (1923).

[28] V. Efimov, Yad. Fiz., **12**, 1080 (1970); Sov. J. Nucl. Phys. **12**, 589 (1971).

[29] V. Efimov, Phys. Lett. B **33**, 563 (1970).

[30] K. Varga and Y. Suzuki, Phys. Rev. C **52**, 2885 (1995).

[31] Y. Suzuki and K. Varga, *Stochastic Variational Approach to Quantum-Mechanical Few-Body Problems*, Lecture Notes in Physics, Vol. m54 (Springer, Berlin, 1998).

[32] A. S. Jensen, D. V. Fedorov, K. Langanke, and H. M. Muller, Proceedings of the International Conference on Exotic Nuclei and Atomic Masses (ENAM5), Ed. by M. de Saint Simon and O. Sorlin (Ed. Frontieres, Gif-sur-Yvette, 1995), p. 677.

[33] R. Higa and H.-W. Hammer, and U. van Klock, Nucl. Phys. **A 809**, 171 (2008).

[34] P. Naidon and S. Endo, Rep. Prog. Phys. **80**, 056001 (2017).

[35] J. Mitroy, S. Bubin, W. Horiuchi, Y. Suzuki, L. Adamowicz, W. Cencek, K. Szalewicz, J. Komasa, D. Blume, and K. Varga, Rev. Mod. Phys. **85**, 693-749 (2013).

[36] Y. Suzuki and W. Horiuchi, *Emergent Phenomena in Atomic Nuclei from Large-scale Modeling: A Symmetry-Guided Perspective"* (World Scientific, Singapore, 2017), Chap. 7, pp. 199-227.

[37] Y. Suzuki, W. Horiuchi, M. Orabi, and K. Arai, Few-Body Syst. **42**, 33 (2008).

[38] S. Ali and A. R. Bodmer, Nucl. Phys. **80**, 99 (1966).

[39] B. Buck, H. Friedrich, and C. Wheatley, Nucl. Phys. **A 275**, 246 (1977).

[40] M. Theeten, D. Baye, and P. Descouvemont, Phys. Rev. C **74**, 044304 (2006).

[41] D. V. Fedorov and A. S. Jensen, Phys. Lett. **B 389**, 631 (1996).

[42] F. Ajzenberg-Selove, Nucl. Phys. **A 506**, 1 (1990).

[43] Y. Suzuki and M. Takahashi, Phys. Rev. C **65**, 064318 (2002).

[44] Y. Funaki, H. Horiuchi, and A. Tohsaki, Prog. Part. Nucl. Phys. **82**, 78 (2015).

[45] S. Saito, Prog. Theor. Phys. Suppl. **62**, 11 (1977).

[46] Y. Suzuki and W. Horiuchi, Phys. Rev. C **95**, 044320 (2017).

[47] D. D. Clayton, *Principles of Stellar Evolution and Nucleosynthesis* (McGraw-Hill, New York, 1968).

[48] D.G. Yakovlev and D.A. Shalybkov, Astrophys. Space Phys. Rev. **7**, 311 (1989).

[49] D. Kushnir, E. Waxman, and A. I. Chugunov, Mon. Not. R. Astron. Soc. **486**, 449 (2019).

[50] S. Ichimaru, Rev. Mod. Phys. **65**, 255 (1993).

[51] W. Horiuchi and Y. Suzuki, Phys. Rev. C **78**, 034305 (2008).

[52] W. Horiuchi and Y. Suzuki, Few-Body Syst. **54**, 2407 (2013).

[53] W. Horiuchi and Y. Suzuki, Phys. Rev. C **87**, 034001 (2013).

[54] J. Carlson, S. Gandolfi, F. Pederiva, S. C. Pieper, R. Schiavilla, K. E. Schmidt, and R. B. Wiringa, Rev. Mod. Phys. **87**, 1067 (2015).

[55] S. Ichimaru, Rev. Mod. Phys. **54**, 1017 (1982).

[56] B. Widom, J. Chem. Phys. **39**, 2808 (1963).

[57] B. Jancovici, J. Stat. Phys. **17**, 357 (1977).

[58] J. Bishop, G. V. Rogachev, S. Ahn, E. Aboud, M. Barbui, A. Bosh, J. Hooker, C. Hunt, H. Jayatissa, E. Koshchiy, R. Malecek, S. T. Marley, M. Munch, E. C. Pollacco, C. D. Pruitt, B. T. Roeder, A. Saastamoinen, L. G. Sobotka and S. Upadhyayula, Phys. Rev. C **103**, L051303 (2021).